

## Atomic Transport and Chemical Stability during Annealing of Ultrathin Al<sub>2</sub>O<sub>3</sub> Films on Si

C. Krug,<sup>1</sup> E. B. O. da Rosa,<sup>1</sup> R. M. C. de Almeida,<sup>1</sup> J. Morais,<sup>1</sup> I. J. R. Baumvol,<sup>1</sup>  
T. D. M. Salgado,<sup>2</sup> and F. C. Stedile<sup>2</sup>

<sup>1</sup>*Instituto de Física, UFRGS, Av. Bento Gonçalves, 9500, Porto Alegre, RS, Brazil 91509-900*

<sup>2</sup>*Instituto de Química, UFRGS, Av. Bento Gonçalves, 9500, Porto Alegre, RS, Brazil 91509-900*  
(Received 14 June 2000)

Ultrathin films of Al<sub>2</sub>O<sub>3</sub> deposited on Si were submitted to rapid thermal annealing in vacuum or in oxygen atmosphere, in the temperature range from 600 to 800 °C. Nuclear reaction profiling with subnanometric depth resolution evidenced mobility of O, Al, and Si species, and angle-resolved x-ray photoelectron spectroscopy revealed the formation of Si-Al-O compounds in near-surface regions, under oxidizing atmosphere at and above 700 °C. Under vacuum annealing all species remained essentially immobile. A model is presented based on diffusion-reaction equations capable of explaining the mobilities and reproducing the obtained profiles.

PACS numbers: 68.35.Fx, 82.65.-i

The search for an alternative to SiO<sub>2</sub> as the material for gate dielectrics in Si-based devices constitutes a new and very lively research area, as the exponential increase in tunneling current with decreasing film thickness sets a fundamental limit on the scaling of gate oxides [1]. The trend in reducing lateral dimensions of devices brings as a consequence a reduction of the capacitance of the involved metal-oxide-semiconductor structures, thus calling for higher dielectric constant and/or thinner films to compensate. Therefore, to keep device areas small and prevent leakage current while maintaining the same gate capacitance, a thicker film made with a material of higher dielectric constant (high-*K*) is required [1–5]. Previous investigations of some high-*K* oxides deposited on Si demonstrated [3] that a postdeposition annealing at moderate temperatures in dry O<sub>2</sub> can reduce the leakage current and the density of interface states to acceptable limits, without significant lowering of their dielectric constants [1–3]. For most high-*K* materials higher dielectric constant comes at the expense of narrower band gap, which can itself result in leakage. Al<sub>2</sub>O<sub>3</sub> is an exception, since it has a high energy band gap (9 eV) similar to SiO<sub>2</sub> and the dielectric constant is more than twice as high (9 as compared to 3.8 for SiO<sub>2</sub>). Furthermore, capacitance versus voltage characteristics point in the direction of a feasible integration of this material into Si-based technology [4]. This Letter addresses for the first time, to the best of our knowledge, experimental and theoretical investigation of atomic transport and chemical stability of ultrathin, amorphous Al<sub>2</sub>O<sub>3</sub> films deposited on Si substrates when submitted to rapid thermal annealing (RTA) in dry O<sub>2</sub> or in vacuum.

Starting samples were 6.5 nm thick Al<sub>2</sub>O<sub>3</sub> films deposited by atomic layer chemical vapor deposition (ALCVD) on Si(001) substrates [6]. ALCVD is a technique that uses sequential pulses of precursors (trimethylaluminum and water, in the present case) and the self-saturating nature of certain surface reactions

allowing chemically deposited materials with a monolayer control. An ultrathin (less than 1 nm thick) amorphous silicon oxide buffer layer was thermally grown in O<sub>2</sub> on the Si substrates before Al<sub>2</sub>O<sub>3</sub> deposition, aiming at preventing further oxidation of the substrate. RTA was performed either in vacuum ( $5 \times 10^{-7}$  mbar) or under 70 mbar of <sup>18</sup>O-enriched (98.5%) O<sub>2</sub>, termed <sup>18</sup>O<sub>2</sub>, so that the oxygen incorporated could be distinguished from that previously existing in the Al<sub>2</sub>O<sub>3</sub> films. Areal densities of <sup>16</sup>O and <sup>18</sup>O were determined before and after RTA by nuclear reaction analysis [7]. Atomic transport was accessed using narrow nuclear resonance profiling (NNRP) [7]. Depth resolutions near the sample surface were ~0.5 nm for <sup>27</sup>Al [4,5] and ~0.7 nm for <sup>29</sup>Si and <sup>18</sup>O [7]. Angle-resolved x-ray photoelectron spectroscopy (XPS) analysis was performed using an OMICRON UHV station based on an EA125 hemispherical analyzer, with an overall resolution of 0.9 eV [5].

The <sup>27</sup>Al profiles are shown in Fig. 1 (top), evidencing (i) constant Al concentration in the as-deposited film corresponding to stoichiometric Al<sub>2</sub>O<sub>3</sub>, as well as an abrupt interface with the substrate [4], within the accuracy and depth resolution of the technique, and (ii) the progressive loss of Al from the surface and interface regions of the films as temperature and time of RTA in O<sub>2</sub> are increased. Since Al does not penetrate into the substrate, this loss must occur through the external surface. After RTA in O<sub>2</sub> at 800 °C for 30 s there is an overall loss of ~25% of the Al atoms.

Areal densities of <sup>18</sup>O and <sup>16</sup>O after RTA in <sup>18</sup>O<sub>2</sub> are given in Table I, evidencing that <sup>18</sup>O is progressively incorporated into the films as RTA temperature and time increase, while <sup>16</sup>O is lost. The <sup>18</sup>O profiles are shown in Fig. 1 (center), indicating the incorporation of <sup>18</sup>O mainly in near-surface regions (~7%), decreasing deeper into the structure. RTA at higher temperatures also leads to the incorporation of some <sup>18</sup>O in the Si substrate, although in smaller amounts than in the Al<sub>2</sub>O<sub>3</sub> film. The <sup>29</sup>Si

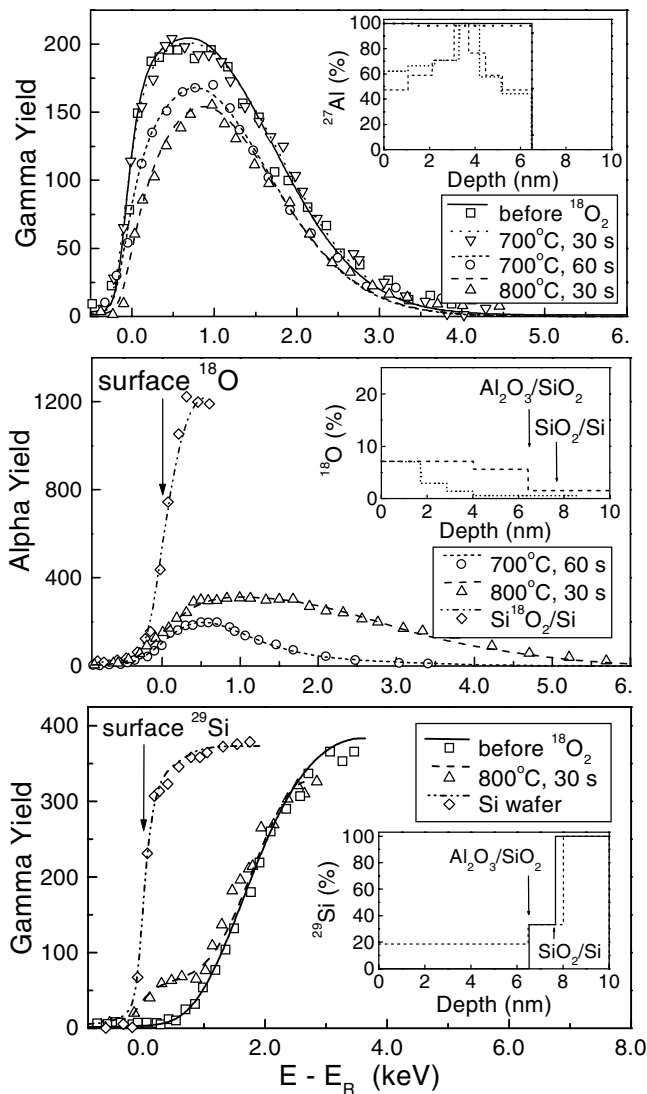


FIG. 1. Excitation curves of the  $^{27}\text{Al}(p, \gamma)^{28}\text{Si}$  (top),  $^{18}\text{O}(p, \alpha)^{15}\text{N}$  (center), and  $^{29}\text{Si}(p, \gamma)^{30}\text{P}$  (bottom) nuclear reactions around resonance energies, with the corresponding profiles in the insets for ultrathin  $\text{Al}_2\text{O}_3/\text{SiO}_2/\text{Si}$  structures submitted to RTAs in  $^{18}\text{O}_2$ . 100% of  $^{27}\text{Al}$ ,  $^{18}\text{O}$ , and  $^{29}\text{Si}$  correspond, respectively, to their concentrations in  $\text{Al}_2\text{O}_3$ ,  $\text{Al}_2^{18}\text{O}_3$ , and Si. Excitation curves from a standard  $\text{Si}^{18}\text{O}_2$  film and from a virgin Si wafer are also shown, in order to determine the surface energy positions of  $^{18}\text{O}$  and  $^{29}\text{Si}$ , respectively. The arrows in the insets indicate the positions of the interfaces before RTA.

profiles in Fig. 1 (bottom) show migration of Si into the  $\text{Al}_2\text{O}_3$  films. This mobility was observed after RTA in  $\text{O}_2$  at 700 and 800 °C, whereas at 600 °C Si movement is negligible or absent. The  $^{18}\text{O}$  and  $^{29}\text{Si}$  profiles reported here evidence a different oxidation mechanism of ultrathin  $\text{Al}_2\text{O}_3/\text{SiO}_2/\text{Si}$  structures as compared to  $\text{SiO}_2/\text{Si}$  [7,8].

Figure 2 shows photoelectron spectra recorded at different take-off angles for samples submitted to RTAs in  $^{18}\text{O}_2$ . At a given take-off angle, the increase in temperature leads to the decrease of the Al  $2p$  peak. This decrease

TABLE I. Areal densities of  $^{18}\text{O}$  incorporated in the  $\text{Al}_2\text{O}_3/\text{SiO}_2/\text{Si}$  structures during RTAs in  $^{18}\text{O}_2$  and the corresponding areal densities of  $^{16}\text{O}$  remaining in these structures. The areal density of  $^{16}\text{O}$  in the as-deposited sample was  $41.2 \times 10^{15} \text{ cm}^{-2}$ .

Temperature (°C)	Areal density ( $10^{15} \text{ cm}^{-2}$ )			
	$^{16}\text{O}$		$^{18}\text{O}$	
	30 s	60 s	30 s	60 s
600	40.6	39.8	0.17	0.40
700	39.6	38.1	0.62	1.36
800	36.5	—	3.65	—

is more pronounced at higher take-off angles, meaning that Al is lost mainly from near-surface regions, thus corroborating NRP results. Concomitantly, two peaks become more pronounced in the Si  $2p$  region, one corresponding to Si bonded to other Si atoms (substrate) and another one near the binding energy corresponding to  $\text{SiO}_2$ . Figure 3 presents in detail the Si  $2p$  region for the sample treated at 800 °C for 30 s. As the analysis becomes more sensitive to the surface, the substrate-Si signal decreases, whereas the near- $\text{SiO}_2$  signal becomes more prominent, indicating that this last environment is more abundant in near-surface regions of the films. This second, broad peak does not correspond exactly to Si bonded only to oxygen atoms. The lower binding energy contribution indicates that Si is bonded to an atom that has a lower electronegativity than O, namely, Al. Thus we attributed this peak centered at 102.5 eV to either aluminum silicate [5], some other Si-Al-O compound, or  $\text{SiO}_2\text{-Al}_2\text{O}_3$  phase mixture.

In summary, the experimental evidences are that, during RTA in  $^{18}\text{O}_2$ , (i) the  $\text{Al}_2\text{O}_3/\text{SiO}_2/\text{Si}$  structures incorporate  $^{18}\text{O}$  in slightly smaller amounts than they lose  $^{16}\text{O}$ , (ii) aluminum moves towards the surface where it leaves the film in higher amounts than  $^{16}\text{O}$  is lost, and (iii) silicon migrates towards the surface reacting in the region that was formerly an aluminum oxide film. The same  $\text{Al}_2\text{O}_3/\text{SiO}_2/\text{Si}$  structures were submitted to RTA in high vacuum at the same temperatures and times. In all cases,  $^{16}\text{O}$  was not lost, and  $^{27}\text{Al}$  and  $^{29}\text{Si}$  profiles before and after RTA were superimposable, evidencing immobility of all species (and the absence of Al loss). Furthermore, a sample annealed in vacuum (700 °C, 120 s) followed by annealing in  $^{18}\text{O}_2$  (800 °C, 30 s) reproduced the results observed in the sample annealed in  $^{18}\text{O}_2$  (800 °C, 30 s) only. It thus became evident that oxygen from the gas phase plays an essential role in promoting atomic transport and chemical reactions during thermal annealing.

A diffusion-reaction [9] model can be proposed if one considers O, Al, and Si in two different states: mobile and fixed. In the case of oxygen, the mobile state corresponds mainly to  $\text{O}_2$  diffusing during RTA in  $\text{O}_2$ , while, in the case of Al or Si, it corresponds to interstitially

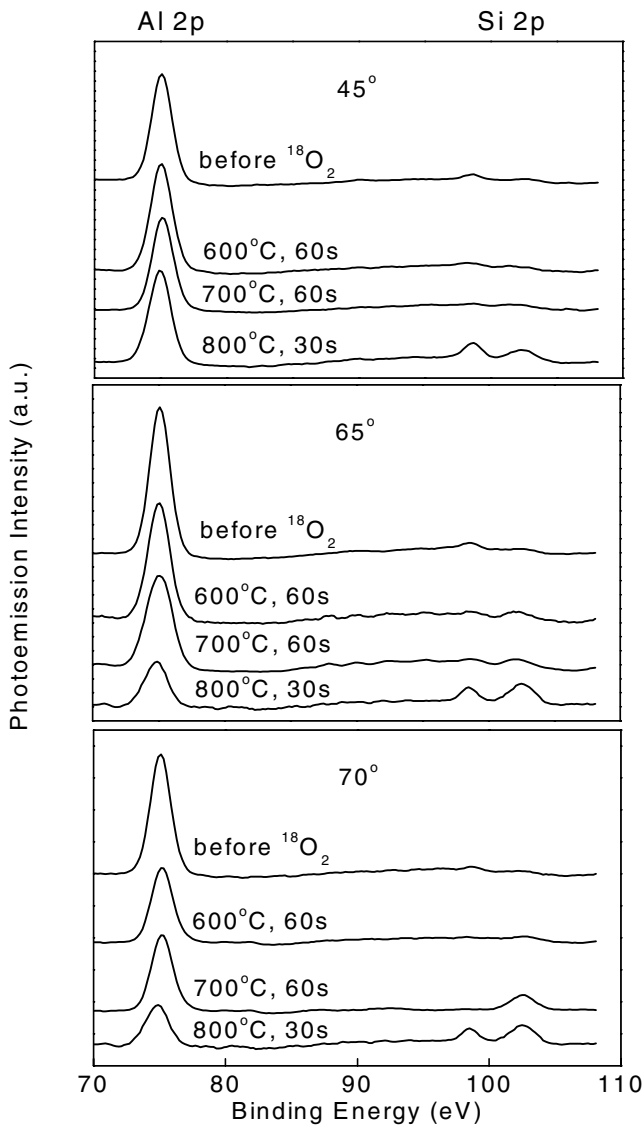


FIG. 2. XPS spectra (a.u. = arbitrary units) showing the Al 2*p* and Si 2*p* photoelectron peak regions for different take-off angles (between surface normal and the electron energy analyzer axis) of Al<sub>2</sub>O<sub>3</sub>/SiO<sub>2</sub>/Si structures submitted or not to RTAs in <sup>18</sup>O<sub>2</sub>.

positioned atoms. Local densities of these species at any time can be described by their relative atomic concentrations  $\rho_i(x, t) = C_i(x, t)/C_{\text{Si}}^{\text{bulk}}$ , where  $C_i(x, t)$  is the concentration of the  $i$ th species (O fixed or diffusive, Al fixed or interstitial, and Si fixed or interstitial) and  $C_{\text{Si}}^{\text{bulk}}$  is Si concentration in bulk, crystalline Si;  $x$  measures the depth from the surface and  $t$  measures the elapsed time. The density functions are hence dimensionless and imply a mean field approximation, since they are functions of depth only.

We assume an initial layer of stoichiometric Al<sub>2</sub>O<sub>3</sub> with thickness  $\Delta x_1$  on a thin layer of SiO<sub>2</sub> ( $\Delta x_2$  thick) on a Si substrate. Before RTA, the density functions for the fixed species are different from zero at

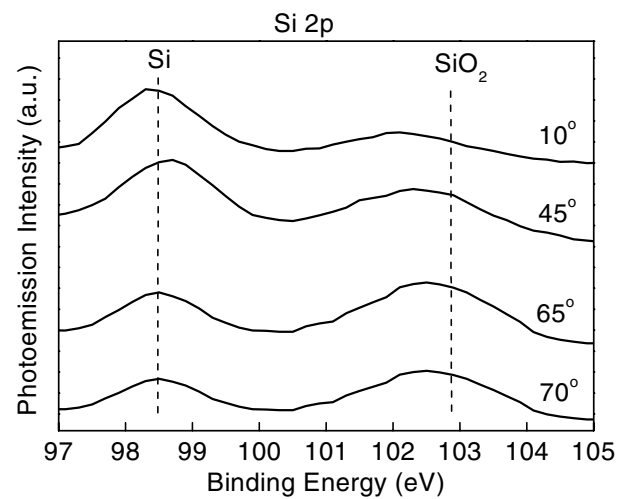


FIG. 3. XPS spectra for the sample submitted to RTA in <sup>18</sup>O<sub>2</sub> at 800 °C for 30 s, showing the Si 2*p* region for different take-off angles. The dashed lines indicate the binding energies of Si atoms bonded only to Si (substrate Si) and of Si bonded only to oxygen atoms (SiO<sub>2</sub>).

$$\begin{aligned} \rho_{\text{Al}}^f(x, 0) &= 1.0 \quad \text{for } 0 \leq x \leq \Delta x_1, \\ \rho_{\text{O}}^f(x, 0) &= \begin{cases} 1.5 & \text{for } 0 \leq x \leq \Delta x_1 \\ 1.0 & \text{for } \Delta x_1 \leq x \leq (\Delta x_1 + \Delta x_2) \end{cases} \quad (1) \\ \rho_{\text{Si}}^f(x, 0) &= \begin{cases} 0.5 & \text{for } \Delta x_1 \leq x \leq (\Delta x_1 + \Delta x_2) \\ 1.0 & \text{for } x \geq (\Delta x_1 + \Delta x_2) \end{cases} \end{aligned}$$

where  $f$  stands for the corresponding fixed states. Here Si concentration in SiO<sub>2</sub> is taken as half the value of either Si concentration in Si or Al concentration in Al<sub>2</sub>O<sub>3</sub>, according to approximate densities of these materials. Fixed O concentrations are taken by assuming that both oxide layers are initially fully oxidized. The normalization condition, reflecting volume conservation in each layer, is  $\rho_{\text{Al}}^f + 2\rho_{\text{Si}}^f - \rho_{\text{Si}}^{\text{nof}} = 1$ , where  $\rho_{\text{Si}}^{\text{nof}}$  is the nonoxidized fraction of fixed Si.

The following scenario thus emerges: the initial structure Al<sub>2</sub>O<sub>3</sub>/SiO<sub>2</sub>/Si is exposed to O<sub>2</sub> at a given pressure  $P_{\text{O}}$ . Oxygen diffuses through the initial oxides, being eventually exchanged for O already existent in these films. Upon reaching bulk silicon, it reacts by forming silicon oxide. As oxidized Si occupies a larger volume, it also generates interstitial Si that is prone to move [10]. Hence, silicon oxidation has a twofold effect: it transforms oxygen from mobile to fixed and some silicon from fixed to mobile species. Mobile silicon spreads through the sample, towards both bulk Si and Al<sub>2</sub>O<sub>3</sub> regions. Interstitial Si cannot be trapped in SiO<sub>2</sub> [11]. However, when in the Al<sub>2</sub>O<sub>3</sub> region, mobile Si may displace Al, since silicon oxide formation is thermodynamically favored over that of aluminum oxide. This reaction implies fixing Si in the original Al<sub>2</sub>O<sub>3</sub> region and transferring fixed Al and O from the Al<sub>2</sub>O<sub>3</sub> network to mobile states. Mobile Al and O atoms that reach

the surface may escape, reducing their total amounts in the sample. Since interstitial Si is generated by oxidation of Si and interstitial Al is created by reaction involving interstitial Si, in the absence of Si oxidation there is neither Si and Al transport nor Al loss. Therefore, the experimental observation that annealing in vacuum does not change the initial profiles is consistent with the depicted scenario.

The differential equations for the density functions are

$$\begin{aligned}
 \frac{\partial \rho_O^d}{\partial t} &= D_1 \frac{\partial^2 \rho_O^d}{\partial x^2} - 2k_1 \rho_{Si}^{nof} \rho_O^d + k_2 \rho_{Si}^i \rho_{Al}^f, \\
 \frac{\partial \rho_O^f}{\partial t} &= 2k_1 \rho_{Si}^{nof} \rho_O^d - k_2 \rho_{Si}^i \rho_{Al}^f, \\
 \frac{\partial \rho_{Si}^i}{\partial t} &= D_2 \frac{\partial^2 \rho_{Si}^i}{\partial x^2} + k_1 \rho_{Si}^{nof} \rho_O^d - k_2 \rho_{Si}^i \rho_{Al}^f, \\
 \frac{\partial \rho_{Si}^f}{\partial t} &= -k_1 \rho_{Si}^{nof} \rho_O^d + k_2 \rho_{Si}^i \rho_{Al}^f, \\
 \frac{\partial \rho_{Al}^i}{\partial t} &= D_3 \rho_{Al}^f \frac{\partial^2 \rho_{Al}^i}{\partial x^2} - D_3 \rho_{Al}^i \frac{\partial^2 \rho_{Al}^f}{\partial x^2} + 2k_2 \rho_{Si}^i \rho_{Al}^f, \\
 \frac{\partial \rho_{Al}^f}{\partial t} &= -2k_2 \rho_{Si}^i \rho_{Al}^f,
 \end{aligned}
 \tag{2}$$

where *d* and *i* stand, respectively, for diffusive and interstitial species.  $D_1$  and  $D_2$  are the diffusivities of mobile O and Si, respectively (assumed to be the same in all materials), while  $D_3$  is the diffusivity of interstitial Al through  $Al_2O_3$  [Fig. 1 (top) shows that Al is present only in the  $Al_2O_3$  region] [12].  $k_1$  and  $k_2$  are, respectively, reaction rates for Si oxidation and for Al displacement by interstitial Si.

Initial conditions are given by Eqs. (1) together with  $\rho_O^d(x, 0) = \rho_{Si}^i(x, 0) = \rho_{Al}^i(x, 0) = 0$ . Boundary conditions are such that a constant oxygen pressure is kept at the surface [ $\rho_O^d(0, t) = P_O$ ] and interstitial Al flux is free through the surface [ $\rho_{Al}^i(0, t) = 0$ ].

Equations (2) were solved by a finite-difference method yielding density function profiles (shown in Fig. 4) considering suitable values for the parameters. The profiles reproduce the experimental results, with (i) aluminum being lost and its profile ( $Al^f + Al^i$ ) presenting a maximum between surface and interface, (ii) silicon migrating into the aluminum oxide region, forming a compound containing Si, Al, and O, (iii) a slight growth of the silicon oxide layer, and (iv) fixed oxygen being partially lost from the Al-rich region in amounts that equal one-half of the amounts of lost Al.

In conclusion, the experiments reported here evidenced the mobility and reaction of Al, O, and Si during RTA of  $Al_2O_3/SiO_2/Si$  nanostructures in  $O_2$  and their immo-

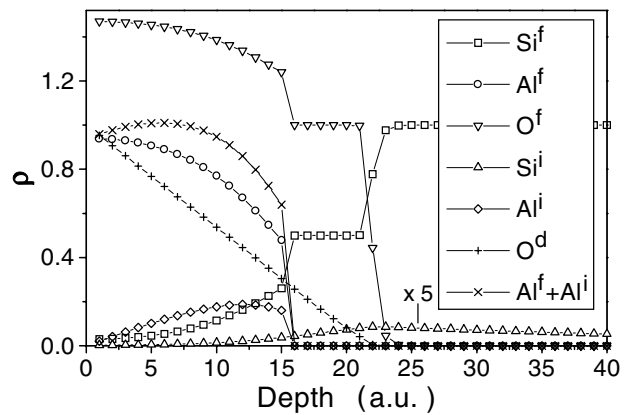


FIG. 4. Calculated density function profiles for all species and for the sum of both aluminum species after 15 000 iterations. Interstitial Si profile was multiplied by a factor of 5.

bility during annealing in vacuum. A diffusion-reaction model is able to semiquantitatively reproduce the profiles of the involved species. In order to obtain more realistic values for the parameters of the model equations as well as quantitative profiles, further experiments are being accomplished, especially concerning the dependence of the profiles on annealing time.

- 
- [1] D. A. Buchanan, *IBM J. Res. Dev.* **43**, 245 (1999).  
 [2] M. C. Gilmer *et al.*, in *Ultrathin SiO<sub>2</sub> and High-K Materials for ULSI Gate Dielectrics*, edited by H. R. Huff *et al.*, MRS Symposia Proceedings (Materials Research Society, Warrendale, 1999), Vol. 567, pp. 323–341.  
 [3] C. Chaneliere, J.L. Autran, R.A.B. Devine, and B. Balland, *Mater. Sci. Eng.* **R22**, 269 (1998).  
 [4] E. P. Gusev *et al.*, *Appl. Phys. Lett.* **76**, 176 (2000).  
 [5] T. M. Klein *et al.*, *Appl. Phys. Lett.* **75**, 4001 (1999).  
 [6] T. Suntola, *Appl. Surf. Sci.* **100/101**, 391 (1996).  
 [7] I. J. R. Baumvol, *Surf. Sci. Rep.* **36**, 1 (1999).  
 [8] I. J. R. Baumvol *et al.*, *Phys. Rev. B* **60**, 1492 (1999).  
 [9] R. M. C. de Almeida, S. Gonçalves, I. J. R. Baumvol, and F. C. Steidle, *Phys. Rev. B* **61**, 12992 (2000).  
 [10] A. Pasquarello, M. S. Hybertsen, and R. Car, *Nature (London)* **396**, 58 (1998).  
 [11] R. E. Walkup and S. I. Raider, *Appl. Phys. Lett.* **53**, 888 (1988).  
 [12] The origin of the second derivatives in the equation for  $\rho_{Al}^i$  in Eqs. (2) is in the finite difference version of the equation for  $x > 0$ :  $\rho_{Al}^i(x, t + \Delta t) - \rho_{Al}^i(x, t) = D_3 \frac{\Delta t}{(\Delta x)^2} \{ \rho_{Al}^f(x, t) [ \rho_{Al}^i(x - \Delta x, t) + \rho_{Al}^i(x + \Delta x, t) ] - \rho_{Al}^i(x, t) [ \rho_{Al}^f(x - \Delta x, t) + \rho_{Al}^f(x + \Delta x, t) ] \} + 2k_2 \Delta t \times \rho_{Si}^i(x, t) \rho_{Al}^f(x, t)$ , that is,  $Al^i$  may only move to regions where there is  $Al^f$ .